Large, tunable and reversible pH changes by spiropyran photoacids

Laura Wimberger,[†] Shyamal K. K. Prasad,[†] Joakim Andréasson,[‡] Timothy W. Schmidt,[†] Jonathon E. Beves[†,*]

Photoswitch, photochromic, spiropyran, photoacid, molecular switch.

ABSTRACT: Molecular photoswitches capable of generating pH changes with precision will allow pH-dependent processes to be controlled remotely and non-invasively with light. We introduce a series of new spiropyran photoswitches, delivering reversible bulk pH changes up to 3.2 pH units (pH 6.5 to pH 3.3) upon irradiation with 450 nm light, displaying tunable and predictable timescales for thermal recovery. We present models to show that the key parameters for optimizing the bulk pH changes are measurable: the solubility of the photoswitch, the acidity of the merocyanine form influenced by the thermal equilibrium position between the spiropyran and the merocyanine isomers, and the increased acidity under visible light irradiation. Using ultrafast transient absorption spectroscopy, we determine quantum yields for the ring closing reaction and observe the lifetime of the transient *cis*-merocyanine isomer ranging from 30 to 550 ns. Quantum yields did not appear to be a limitation of bulk pH switching. The models we present use experimentally determined parameters and are, in-principle, able to predict the change in pH obtained for any related spiropyran photoacid.

INTRODUCTION

Controlling pH environments is critical for many important chemical processes, including the biological operating ranges of enzymes and using proton gradients for energy storage. Tools for reversible pH control are highly sought-after for mimicking biological systems and to control chemical processes like catalysis,[1] assembly/disassembly,[2] generating out-of-equilibrium states,[3] or controlling molecular machines.[4] It has long been recognised[5] that using light to reversibly control pH has the advantage of being non-invasive and allows precise control in both time and space. One way to use light to control pH is with molecular photoacids. Photoacids are molecules whose excited states are substantially more acidic than the ground state. For example 8-hydroxypyrene-1,3,6-trisulfonic acid (HPTS) exhibits a very large change in pK_a from the ground state (pK_a = 7.3) to the excited state (pK_a = 1.4).[6,7] The short lifetimes of excited states, e.g. 6 ns for HPTS,[7] prevent buildup of a significant proton concentration and the resulting pH changes are limited, although some impressive applications have been reported.[8] Molecules that can be isomerized by visible light to long-lived *metastable* ground states are more suitable for controlling many protonation/deprotonation events.[9] Photoacids based on the spiropyran photoswitch[10] are generally the most versatile and widely used in part due to the large difference in effective pK_a between the spiropyran (SP) and merocyanine (MC(H)) forms (Fig. 1).

The first spiropyran commonly used as a reversible photoacid was ethylene alcohol functionalized spiropyran **1**.[11] This photoswitch was used in organic solvents for controlling self-assembly,[12] luminescence[13] and optical signaling.[14] However, the relatively slow thermal recovery time (several days)[11b] and poor solubility of the spiropyran form in water[15] limited more widespread applications.

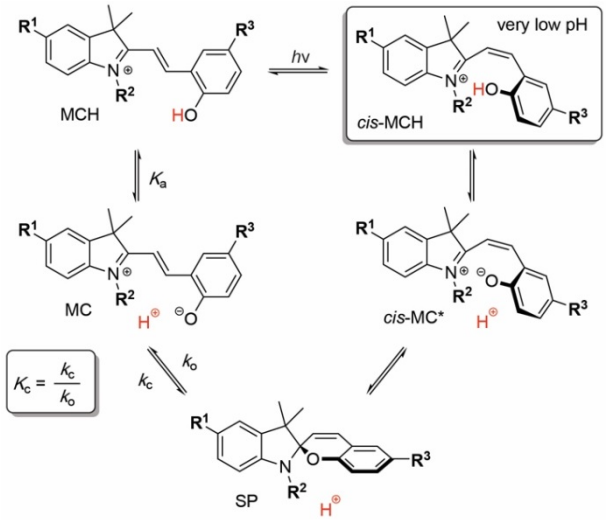

	R^1	R^2	R^3	Ref.
1	H	$(CH_2)_2OH$	NO_2	Ref. 11
2a	H	$(CH_2)_3SO_3^-$	H	Ref. 16a / Ref. 31 / This work
2b	H	$(CH_2)_3SO_3^-$	*t*Bu	This work
2c	OMe	$(CH_2)_3SO_3^-$	*t*Bu	This work
3a	H	$(CH_2)_3NMe_3^+$	H	This work
3b	H	$(CH_2)_3NMe_3^+$	*t*Bu	This work
3c	OMe	$(CH_2)_3NMe_3^+$	*t*Bu	This work
3d	OMe	$(CH_2)_3NMe_3^+$	H	This work

Figure 1. The spiropyran photoacid (photo)thermal equilibrium of photoacids **2a–3d** prepared in this study. The *cis*-MC* isomer is a transient species.

Liao[16] introduced a sulfonate group at the end of an alkyl chain attached to the indolinium nitrogen (position R^2, Fig. 1) to prepare water-soluble spiropyran **2a.**[17] This photoacid allowed bulk pH switching by ~2 pH units (pH 5.5 to 3.5), with a thermal half-life of 70s for the pH recovery in the dark. The large jump in pH and the relatively rapid thermal recovery allowed this photoswitch to be applied in

diverse contexts. Examples are controlling self-assembly of discrete[18] or extended structures,[19,18d] including DNA structures[3c,20] or nanoparticles,[21] and influencing the properties of nanoreactors,[22] soft materials,[23] gels[24] and dyes.[25] Other applications include the control of polymerizations,[26] hydrazone molecular switches,[27] enhancing photophosphorylation by chloroplasts,[28] and operating molecular machines.[29] Building on earlier investigations,[30] Pezzato and co-workers recently reported a detailed study that significantly progressed the understanding of the thermodynamic and kinetic parameters of photoacid **2a.**[31] Using optimized conditions, the authors demonstrated a 2.5 unit pH jump (~6.1 to ~3.6 pH)[31] and very recently improved it to approximately 3 pH units (~7 to ~4 pH).[32]

Despite these advances, designing spiropyran photoacids for desired pH changes remains a significant challenge as the observed pH jump depends on several chemical/photophysical properties for which the structure-property relationships are not fully understood. Here we introduce spiropyrans **2b**–**3d** to investigate their photoacidic properties, and identify key parameters which are responsible for the limits on bulk pH switching by spiropyrans, providing clear guidelines for their ideal application, and highlighting their limitations.

In the dark, spiropyran photoacids exist predominantly in three forms:[10] protonated merocyanine (MCH), deprotonated merocyanine (MC) and spiropyran (SP), see Fig. 1. The MC undergoes thermal ring closing (rate constant k_c) to form SP which can ring open (rate constant k_o) in the reverse reaction to give an equilibrium constant K_c, as in Eqn. 1.

$$K_c = \frac{[SP]}{[MC]} = \frac{k_c}{k_o} \qquad \text{(Eqn. 1)}$$

The thermal equilibrium between MC and SP (K_c) is inherently linked to the protonation equilibrium (K_a) between MCH and MC, Eqn. 2.

$$K_a = \frac{[MC][H^+]}{[MCH]} \qquad \text{(Eqn. 2)}$$

At pH values where MC is preferentially protonated, MCH is thermodynamically stable and the equilibrium can be shifted entirely to the MCH form at sufficiently low pH.[33] Under visible light irradiation the MCH undergoes *trans* to *cis* isomerization[34] forming *cis*-MCH which is reportedly more acidic than MCH.[31,35] Thus, *cis*-MCH can only be observed at very low pH.[36,31] The deprotonation to *cis*-MC leads to fast ring closure to the SP form,[35] resulting in increased proton concentrations under irradiation and as such acting as a photoacid.

RESULTS AND DISCUSSION

We synthesized a small library of spiropyrans **2a–c, 3a–d** in two or three steps (for details of preparation and characterization see SI-S2-S4) and used reported[31] **2a** as a reference compound. Substituents were introduced in three different positions (Fig. 1, R^1, R^2 and R^3) to study their effects on the proton dissociation behavior. An increase in pK_a values is desired as this would allow applications near neutral pH values. We opted for unsubstituted phenolic moieties or substitution with a weakly electron-donating group (R^3 = *t*Bu). This is to prevent a decrease of the pK_a value which occurs for substitution with electron-withdrawing groups that can stabilize the negative charge on the phenolate oxygen.[16a,33a,10a] Introducing a methoxy group on the indolinium ring (R^1= OMe) has been reported[37] to increase the pK_a value, so we included examples in our study to explore this effect. Very recently, it was also shown that the introduction of a methoxy group in this position improves the hydrolytic stability.[32] We studied the effects of the alkyl side chain (R^2) by comparing a negatively charged sulfonate group and a positively charged trimethyl ammonium group.[33a] To determine the change in acidity upon light irradiation of our spiropyrans we applied a recently reported methodology by Pezzato and co-workers.[31] A series of equilibrated UV-visible absorption spectra were collected at different pH values in the dark and under visible light irradiation. Representative data for photoacid **3d** are shown in Fig. 2. The data was fit to a sigmoidal function[31] to determine the acidity in the dark, pK_a^{dark}, and under irradiation, p$K_a^{h\nu}$ defined as (see SI-S5.5 for details):

$$K_a^{dark} = \frac{[H^+]([MC]+[SP])}{[MCH]} = K_a(1 + K_c) \qquad \text{(Eqn. 3)}$$

$$K_a^{h\nu} = \frac{[H^+][SP]}{[cis\text{–}MCH]} \qquad \text{(Eqn. 4)}$$

The photoacidity Π is calculated[31] as the difference between pK_a^{dark} and p$K_a^{h\nu}$. The values obtained for all compounds are shown in Table 1. Photoacid **2a** served as a reference compound and our obtained values are in good agreement with the literature.[31] The experimentally observed pK_a^{dark} value is *not* equivalent to the pK_a value of the MCH form, as previously noted.[31] The pK_a^{dark} value considers the K_a and the K_c equilibria since the deprotonation of MCH to MC is linked to the ring closure to form SP. This implies that pK_a^{dark} approaches pK_a of MCH when the equilibrium shifts sufficiently towards MC (i.e. K_c ~0, [SP] ~0), or if the rate of ring closure is very slow (i.e. low k_c). In all other cases the shift in the equilibrium toward the SP form (i.e. $K_c\uparrow$) leads to a decrease in the pK_a^{dark} value with respect to the pK_a value of MCH (i.e. p$K_a^{dark} \leq$ pK_a). As far as we are aware, many previously reported "pK_a" values of merocyanines are pK_a^{dark} values, unless the above criteria is met (i.e. very low K_c, or very low k_c).

The p$K_a^{h\nu}$ value determined under irradiation can be viewed as the pK_a value of the *cis*-MCH form since the equilibrium between *cis*-MC and SP is shifted entirely to SP when irradiated. The *cis*-MC form is short-lived, and can only be detected by transient absorption spectrosctopy,[35,38] whereas *cis*-MCH is stable at low pH values (determined by p$K_a^{h\nu}$).[39,36] It deserves mentioning that *cis*-MCH has been previously erroneously assigned as the protonated spiropyran (SPH).[40a,33a,10a,40b] This error is easy to make due to the apparent barrierless transition from SP to *cis*-MCH that occurs at low pH,[36] and from a practical perspective *cis*-MCH behaves mechanistically as SPH.

The pK_a^{dark} and p$K_a^{h\nu}$ values obtained for our library of compounds cover a range between 4.52–7.11 for pK_a^{dark} and 1.03–3.72 for p$K_a^{h\nu}$. The introduction of a methoxy group onto the indolinium ring (R^1, Fig. 1) caused an increase of *ca*. 1 unit for both for pK_a^{dark} and p$K_a^{h\nu}$ in all compounds (i.e. **2b** *vs* **2c**; **3a** *vs* **3d**; **3b** *vs* **3c**). By contrast, introducing a *tert*-butyl group (R^3, Fig. 1) had a negligible effect on the pK_a^{dark} and p$K_a^{h\nu}$ values (i.e. **2a** *vs* **2b**; **3a** *vs* **3b**; **3d** *vs* **3c**).

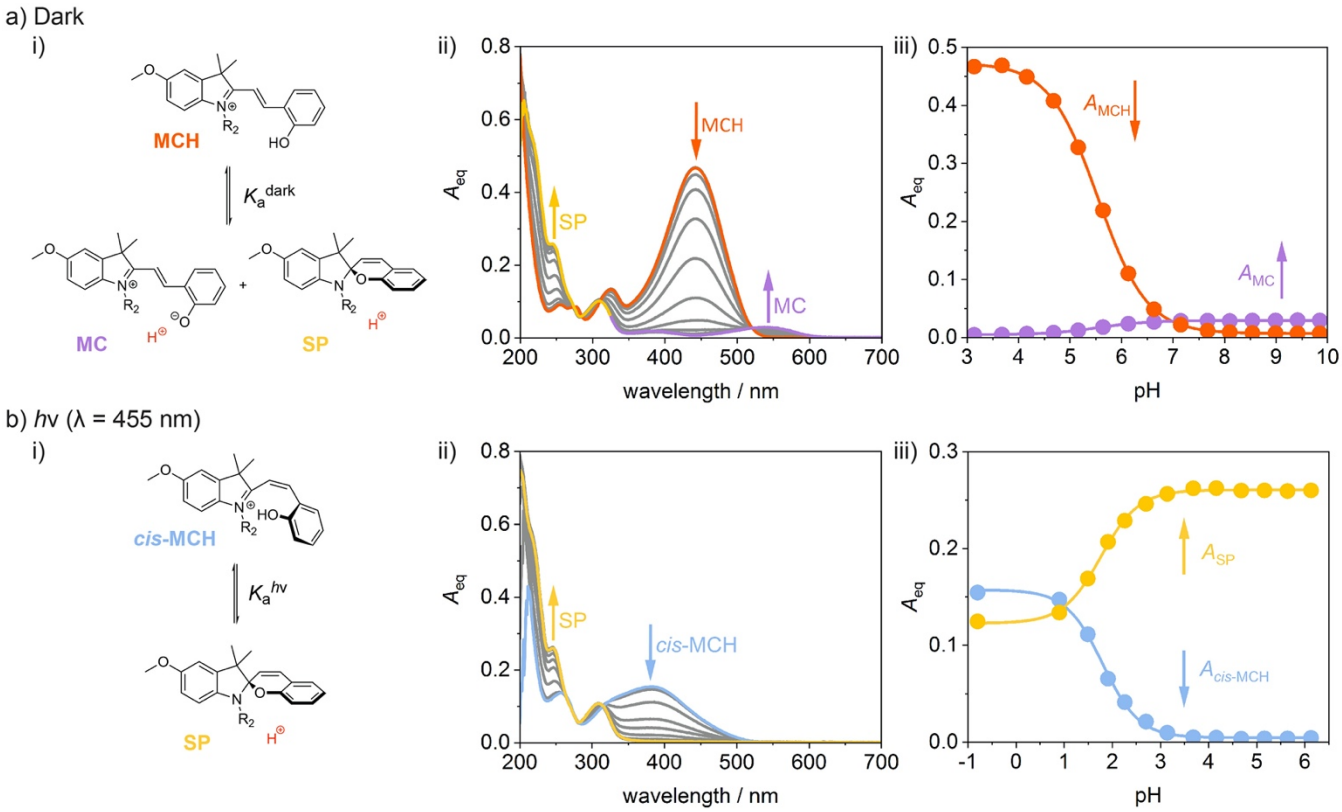

Figure 2. a) pK_a^{dark} determination. i) The K_a^{dark} equilibrium between photoacid **3d**-MCH and the deprotonated forms **3d**-MC and **3d**-SP. ii) Equilibrated UV-vis absorbance spectra of photoacid **3d** in the dark over a pH range (orange: pH = 3.1, yellow/purple: pH = 9.9). iii) The change in absorbance maxima characteristic for the individual species (orange: λ_{MCH} = 442 nm, purple: λ_{MC} = 538 nm) over the pH range with corresponding fits to Eq. S1 (SI-S5.4) to determine pK_a^{dark} (inflection point). Experimental conditions: [**3d**] = 16.3 µM, [phosphate buffer] = 20 mM, pH 2.7–9.9, T = 25 °C. b) p$K_a^{hν}$ determination. i) The $K_a^{hν}$ equilibrium between photoacid **3d**-*cis*-MCH and the deprotonated form **3d**-SP. ii) Equilibrated UV-vis absorbance spectra of photoacid **3d** under blue light irradiation (λ = 455 nm) at different pH values (blue: pH = –0.8, yellow: pH = 6.1). iii) The change in absorbance maxima characteristic for the individual species (yellow: λ_{SP} = 246 nm, blue: $\lambda_{cis\text{-}MCH}$ = 383 nm) over the pH range with corresponding fits to Eq. S1 (SI-S5.4) to determine p$K_a^{hν}$. Experimental conditions: $hν$ (λ = 455 nm), [**3d**] = 16.3 µM, [phosphate buffer] = 20 mM, pH –1.1–6.1, T = 25 °C.

The alkylsulfonate substituted (R^2, Fig. 1) compounds **2a**–**2c** have pK_a^{dark} and p$K_a^{hν}$ values ~1.5–1.7 units higher than alkylammonium substituted photoacids **3a**–**3d**. By removing electron-withdrawing groups (R^3) and adding a methoxy group to the indolinium moiety (R^1) the pK_a^{dark} and p$K_a^{hν}$ values of alkylammonium compounds could be significantly increased. For example, the pK_a^{dark} and p$K_a^{hν}$ values for **3d** are up to 1.3 units higher than those reported for known compounds **6**–**11**[33a] (3.3–4.3 for pK_a^{dark} and 0.4–1.6 for p$K_a^{hν}$). An overview of pK_a^{dark} and p$K_a^{hν}$ values of this study (Table 1) compared to reported values is shown in Fig. 3. Interestingly, modifying the electronic properties by changing the substitution patterns appears to similarly influence pK_a^{dark} and p$K_a^{hν}$, resulting in a relatively constant photoacidity parameter Π (3.4–3.9) for our compounds. The known photoacid **2a** retained the highest Π value of 3.9 units. As we explain later, Π is not the main limiting factor for generating bulk pH changes in aqueous solutions, as other properties like the solubility of the compounds play a substantial role. To better understand the effects of the substitution pattern on pK_a^{dark} values we determined K_c values for photoacids **2a**–**c**, **3a**–**d** followed by calculation of the respective pK_a values. The rate constants of the ring opening/closing reaction (k_o/k_c) of the photoacids were determined by the addition of a sample of each photoacid to buffered solutions and monitoring the equilibration process by UV-vis absorbance spectroscopy. We fit the intensity of the MC (or MCH) visible absorption over time (A_t) to the exponential function given in Eqn. 5 to obtain the observed thermal equilibration rate constant, k_{obs}, at different pH values:

$$A_t = A_{eq} + (A_0 - A_{eq})e^{-k_{obs}t} \qquad \text{(Eqn. 5)}$$

where A_{eq} is the absorption at equilibrium and A_0 is the absorption at the start of the measurement.

The varying degree of protonation coincided with a change in k_{obs} over the pH range (Fig. 6a, see SI-S5.6 for other compounds). At low pH (<< pK_a) k_{obs} is equal to k_o as the ring closing reaction is impeded by protonation of MC forming the thermodynamically stable MCH form.[33a,31] The rate constants for the ring closing reaction (k_c) of photoacids **2a**–**c** were determined following a reported procedure[31] by monitoring the equilibration process at high pH with UV-vis absorbance spectroscopy. At high pH (>> pK_a, [MCH] ~0) the observed rate constant is equal to the sum of the ring closing and ring opening reactions (k_{obs} = k_o + k_c), as expected for a reversible first order process. Photoacids **3a**–**d** have significantly faster rates of ring closing which ruled out application of this method. Instead, we observed the equilibration process by perturbing the

Table 1. Critical parameters of spiropyran photoacids **1**, **2a–c**, **3a–d**.

	pK_a^{dark} [a]	pK_a^{hv} [a]	Π[b]	k_o /10^{-2} s^{-1}	k_c /10^{-2} s^{-1}	K_c [c]	pK_a [d]	$\Phi_{MCH\rightarrow SP}$ [e]
1[f]	4.52[f]	–	–	7.6 × 10^{-3}[f]	–	–	4.52[f]	–
2a	6.27 ± 0.02	2.42 ± 0.04	3.85 ± 0.08	0.54 ± 0.1[h]	2.8 ± 0.5[h]	5.2 ± 1	7.07 ± 0.10	0.11
	(6.19±0.06)[g]	(2.47±0.04)[g]	(3.7±0.1)[g]	(0.45)[g]	(3.9)[g]	(8.6±4.9)[g]	(7.20±0.03)[g]	(0.37±0.04)[g,h]
2b	6.20 ± n.a.	2.81 ± 0.04	3.39 ± 0.04	1.7 ± 0.3[i]	15 ± 3[i]	8.6 ± 2	7.18 ± 0.11	0.04
2c	7.11 ± 0.03	3.72 ± 0.01	3.38 ± 0.03	1.9 ± 0.3[i]	2.3 ± 0.5[i]	1.2 ± 0.3	7.46 ± 0.07	0.16
3a	4.66 ± 0.04	1.03 ± 0.08	3.63 ± 0.09	0.18[j]	22 ± 4[i]	123 ± 23	6.76 ± 0.09	0.06
3b	4.68 ± 0.08	1.20 ± 0.02	3.48 ± 0.08	0.57[j]	104 ± 22[i]	183 ± 40	6.95 ± 0.12	0.03
3c	5.56 ± 0.01	1.98 ± 0.01	3.58 ± 0.01	0.62[j]	25 ± 6[i]	41 ± 10	7.18 ± 0.10	0.11
3d	5.55 ± n.a.	1.78 ± 0.03	3.76 ± 0.03	0.17[j]	4.4 ± 0.9[i]	26 ± 5	6.97 ± 0.08	0.03

[a] pK_a^{dark}: experimentally observed value for the proton dissociation of the MCH form, $pK_a^{dark} \neq pK_a$. pK_a^{hv}: experimentally observed value for the proton dissociation of the photoacids under blue light irradiation (λ = 455 nm), equivalent to the pK_a of *cis*-MCH. pK_a^{dark} and pK_a^{hv} determined from fit to Eq. S1 (SI-S5.4) and reported as average of two fits, error from standard deviation (n.a. = error negligible). [b] Photoacidity parameter: Π = $pK_a^{dark} - pK_a^{hv}$, uncertainty from error propagation. [c] Thermal equilibrium constant describing MC⇌SP as defined in Fig. 1, calculated from Eqn. 1 (SI-S5.6), uncertainty from error propagation. [d] Calculated from Eqn. 6 with pK_a^{dark} experimentally determined from fit to Eq. S1 (SI-S5.4) and K_c from Eqn. 1 (SI-S5.6). [e] Quantum yields for the SP formation from MCH determined by transient absorption (SI-S6). [f] Reported for MCH in water, assuming SP has negligible solubility this value would also be the pK_a see Ref. 15. [g] k_c, k_o and K_c values from Table 1 and Table S1 in Ref. 31. [h] From Ref. 41. [i] k averaged over three temperatures (T = 25 ± 1.5 °C) extracted from linear fit in Eyring plot, errors calculated by standard deviation (details SI-S5.6). [j] Error from single exponential fit is negligible, temperature dependence was not determined.

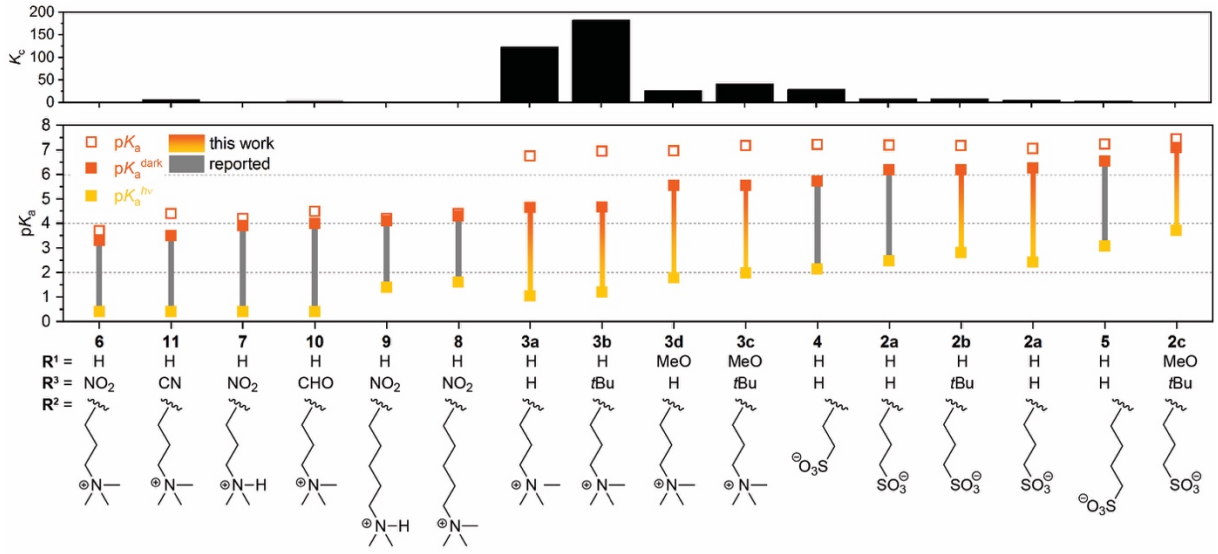

Figure 3. Overview over photoacidity parameters of our study (orange bars) compared to the literature[33a,31] (grey bars): pK_a^{hv} (yellow), pK_a^{dark} (orange) and pK_a (orange box) values of photoacids with their corresponding K_c values shown above.

equilibrium by UV-irradiation at high pH which slightly increased the MC concentration. The resulting changes in concentration of MC were small and the higher time resolution required a custom-made setup (details in the SI-S5.3). The K_c values were then calculated from Eqn. 1. Variable temperature experiments of the equilibration process also allowed us to define a temperature-based error of K_c (see SI-S5.6).

The K_c values of the alkylsulfonate compounds **2a–c** lay in the range of 1–9 and the value for photoacid **2a** agrees with the reported values (5.2 ± 1 *vs* 8.6 ± 4.9, Ref. 31). The K_c value of the alkylammonium compounds **3a–d** are significantly higher, ranging from ~30 to ~180 meaning the SP form is largely preferred over the MC form. The thermodynamic preference of the SP form is related to a decrease in stability of the positive charge on the indolinium nitrogen in the MC/MCH forms. For alkylammonium compounds **3a–d** the positive charge of the sidechain appears to destabilize the positive charge of the indolinium nitrogen leading to an increased relative stability of the SP form (high K_c). By comparison, the negatively charged alkylsulfonate side chain in **2a–c** has a more stabilizing effect on the MC form (lowering K_c). The distance between the charge on the sidechain and that on the indolinium nitrogen has been previously reported to have an influence on the relative stability of the MC form.[33a,31]

Introducing a methoxy group on the indolinium ring (R^1) appears to have a stabilizing effect on the positively charged nitrogen, leading to a decrease in K_c. By contrast, substitution on the phenolic moiety (R^3) has a minimal effect on K_c. For all compounds higher K_c values led to a higher acidity of the system (i.e. $pK_a^{dark}\downarrow$ and $pK_a^{hv}\downarrow$).

The pK_a-values of MCH were calculated from pK_a^{dark} and K_c values by modification of Eqn. 3 to give:

$$pK_a = pK_a{}^{dark} + \log(1 + K_c) \qquad \text{(Eqn. 6)}$$

The obtained pK_a value of 7.07 ± 0.10 for **2a** is in good agreement with the literature reports[31] (7.20 ± 0.03) and

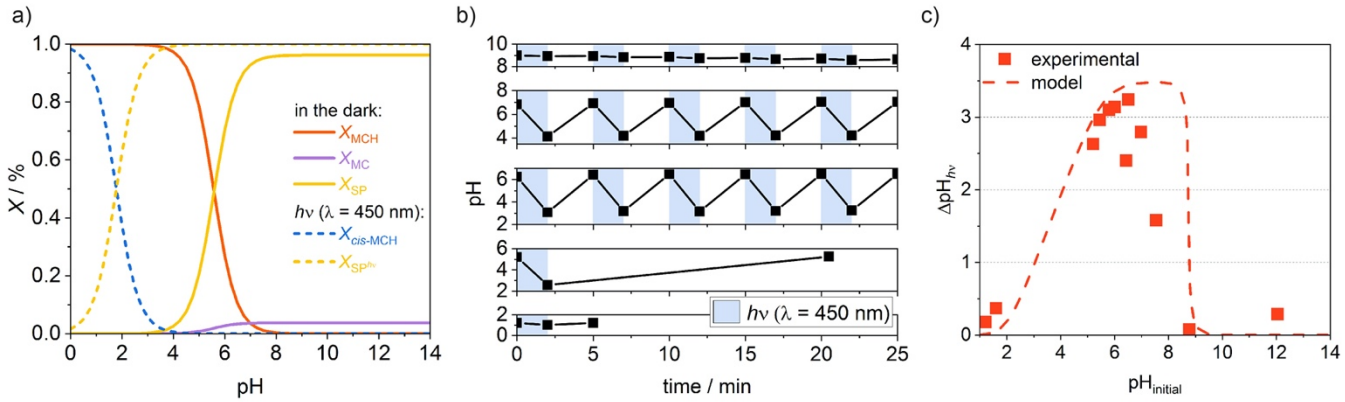

Figure 4. Photoacid **3d**. a) Calculated mole fractions in the dark and under irradiation over the pH range (see SI-S5.7). b) Visible light induced (λ = 450 nm, indicated by blue boxes) pH switching of concentrated aqueous solutions of photoacid **3d** at different initial pH values. c) Experimental pH changes under irradiation ($\Delta pH_{hν}$) achieved at respective initial pH values in comparison to the model predicting pH changes under irradiation.

photoacids **2b–c** have similar values in the range of 7.18–7.46. The pK_a values of **3a–d** are also quite similar (6.76–7.18). Reported spiropyran photoacids[33a] **6–11** have significantly lower pK_a values (3.7–4.5) as they are substituted with electron withdrawing groups on the phenolic ring (Fig. 3, $R^3 = NO_2$, CN, CHO), which stabilizes the negative charge on the phenolate oxygen.

Comparison of our K_c and pK_a values and previously reported ones (Fig. 3, SI-S10.5)[33a,31] suggests that the pK_a value can be tuned by introducing electron donating (pK_a↑) or electron withdrawing groups (pK_a↓) as might be expected. The experimentally observed and "effective" pK_a^{dark} value can be increased by stabilizing the positive charge (K_c↓) on the indolinium nitrogen of the MC form. The maximum achievable pK_a^{dark} is the pK_a value where K_c <<1. For optimized pH switching a small K_c and a high pK_a value are required to result in a high pK_a^{dark} value.

We studied the achievable pH changes caused by the photoacids over a pH range. This requires consideration of following key parameters: 1) the logarithmic scale of pH: higher pH values require smaller concentration of protons to induce a pH change; 2) the autoionization of water K_w at high pH values; 3) the solubility of the photoacid: higher [MCH] will result in higher concentration of released protons upon irradiation; 4) pK_a^{dark}: defines the concentration of MCH present at respective pH values; 5) $pK_a^{hν}$: [*cis*-MCH] under irradiation defines a lower limit of proton dissociation; 6) the extent of photoswitching: full conversion of MCH to SP under irradiation generates the maximum concentration of released protons.

To evaluate the pH switching we first calculated the mole fractions of the individual species (MCH/MC/SP) over the pH range in the dark using pK_a and K_c. The mole fractions under irradiation (*cis*-MCH/SP) were calculated using $pK_a^{hν}$ assuming a complete bleach of the MCH form. The distribution of the individual species over the pH range is shown for photoacid **3d** in Fig. 4a (see SI-S5.7 for data for the other photoacids).

We studied the pH changes of photoacid **3d** which is more soluble (~8 mM) than broadly applied alkylsulfonate derivative **2a** (~0.2 mM). Blue light irradiation (λ = 450 nm) of concentrated solutions of **3d** resulted in a drop of the pH value and in the dark the pH recovered to its initial value making this process fully reversible (Fig. 4b). We adjusted the initial pH of the solution ($pH_{initial}$) by addition of minimal amounts of concentrated acid/base and measured the change in pH upon visible light irradiation at different initial pH values. At low pH the change upon irradiation ($\Delta pH_{hν}$) was minimal due to the high concentration of *cis*-MCH and the large proton concentrations needed to induce a change in pH. As the pH is increased, the light induced pH drop increases, reaching a maximum of more than 3 pH units at an initial pH slightly above its pK_a^{dark} value (5.56). At higher initial pH values the pH drop under irradiation is minimal. These observations confirm that increasing the pK_a^{dark} value allows optimized bulk pH changes as the initial pH value is raised.

The maximum change in pH upon irradiation is due to a correlation between the concentration of MCH and the proton concentration needed to result in a change in pH. The significant reduction of the achievable $\Delta pH_{hν}$ at higher pH can be partially explained by the MCH concentration approaching zero and the released protons favoring protonation of hydroxide ions. At very high pH values (pH~9) blue light irradiation appeared to result in hydrolytic degradation, which is known to occur for spiropyrans.[33,40b,31]

Another crucial aspect at high pH is the increasing relative concentration of MC. Previous transient absorption studies[35] of **2a** indicated excitation of MCH to be the predominant pathway to SP formation, with the MC form having a negligible quantum yield (< 1%) for photoisomerization to SP. Alkylsulfonate[35,38] and alkylammonium spiropyran[42,38] derivatives have been studied previously in the picosecond timescale to elucidate the isomerization mechanism. Excitation of **2a**-MCH was proposed to lead to the *trans* to *cis* isomerization and deprotonation on a picosecond timescale.[35] Depending on the orientation of the phenolic moiety in the *cis*-MC form, a small proportion was proposed to undergo prompt ring closure to the SP form (within ps).[35] A longer-lived species was identified as the *cis*-MC form which needs to rotate around the single bond to undergo ring closure accounting for the longer lifetime (>>3.5 ns).[35]

We measured the transient absorption of photoacids **2a–c**, **3a–d** from 1 ns to 100 μs at different pH values to ob-

serve the decay of this species and calculate quantum yields of MCH/MC for the SP formation. Representative data of photoacid **3a** is shown in Fig 5. We used aqueous samples at pH values where the MCH form dominates and pumped at 355 nm targeting the MCH absorption band. The decay of the excited state species (Fig. 5a, red) was observed resulting in a spectrum containing only the persistent ground state bleach (Fig 5a, blue).

The respective kinetic traces are shown in Fig 5b. The excited state species with a positive change in optical density (ΔOD) at 520-570 nm decays completely over 100 ns, which we propose to be *cis*-MC, in line with previous assignments.[35] This long-lived excited state species of photoacids **2a–c**, **3a–d** had lifetimes of 30–550 ns, confirming previous estimates for **2a** (≫3.5 ns).[35] The ground state bleach at 420-450 nm persists to at least 100 μs and corresponds to the maximum absorbance of MCH. The persistent ground state bleach indicated the concentration of MCH assumed to form SP and was used to calculate the quantum yields of SP formation for photoacids **2a–c**, **3a–d**. Quantum yields for the isomerization of MCH to SP ranged from 3% for **3b** and **3d** to 16% for **2c**. The quantum yield for **2a** was 11%, previously estimated as 37% by UV-vis absorbance,[41,30-31] albeit with excitation at longer wavelengths.

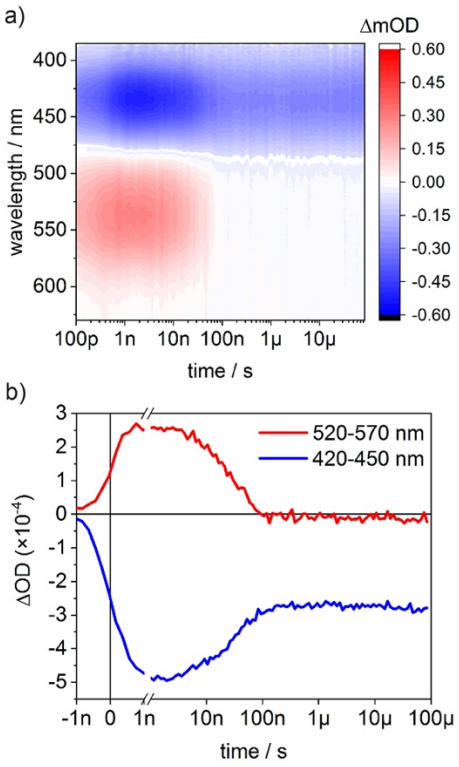

Figure 5. a) Evolution of the transient absorption spectrum of photoacid **3a** following excitation at 355 nm. Experimental conditions: [**3a**] = 16.7 μM, [phosphate buffer] = 20 mM, pH ~3, T = 25 °C. b) Respective kinetic traces averaged over a range of selected wavelengths characteristic for the long-lived excited state species (red) and the ground state bleach (blue).

Similar transient absorption measurements at high pH were used to determine the quantum yields of isomerization by MC. For all compounds these quantum yields were <1%, and within error of zero (SI-S6.3, S7). This confirms that the predominant pathway for photoisomerization is from the MCH form. In addition, our pH switching experiments suggested the isomerization quantum yield of the MCH is not a limiting factor to generate bulk pH changes.

With this data in hand, we developed a model to predict the expected pH changes upon irradiation based on the initial pH value. The solubility, pK_a^{dark} and $pK_a^{h\nu}$ values of the photoacids allow us to predict the pH change upon irradiation at any given initial pH value for any spiropyran with this equilibrium system. Our model assumes the protons contributing to the pH drop solely originate from MCH as well as a complete bleach of MCH upon irradiation (detailed considerations in SI-S10.2).

For photoacid **3d** the model predicts a steady increase of $\Delta pH_{h\nu}$ as the pH value increases (Fig 4c) with a maximum $\Delta pH_{h\nu}$ of ~3.4 reached at an initial pH value of ~8–9, followed by a drastic decrease at higher pH. The model matches the experimental data with reasonable accuracy up to an initial pH value of ~6–7. The model diverges from the experimental data above pH 7 where larger $\Delta pH_{h\nu}$ were predicted at pH values with very low MCH concentration ([MCH] ~0).

Bulk pH switching experiments were also performed with photoacid **3c** (SI-S9.2) which confirmed the general trend of increasing $\Delta pH_{h\nu}$ with increasing initial pH values and a drastic decrease of $\Delta pH_{h\nu}$ at higher pH values (~6). Despite the higher solubility of **3c** (up to ~20 mM) a maximum $\Delta pH_{h\nu}$ of only ~2.7 units was observed experimentally. The model predicted larger $\Delta pH_{h\nu}$ (~3.8) than we found experimentally with a similar discrepancy in shape as for photoacid **3d**. We suspect that the divergence of the model may be attributed to concentration effects, that is aggregation caused by a higher solubility of the compound which is known for other merocyanines.[43]

For application of these spiropyran photoacids the timescale of switching is also of the highest importance. Photoacids **2a–c**, **3a–d** studied here rapidly reached photostationary states at UV-visible absorption concentrations typically within 20–30 seconds and for saturated solutions within 2 min. Therefore, we propose the time-limiting factor for pH switching to be the recovery of pH in the dark after irradiation (Fig. 6b) which is nonlinear over time. This is caused by the evolving rate constant k_{obs} of the SP–MC equilibrium as the pH recovers over time in the dark. We developed a model to describe the pH recovery over time considering the pH dependent parameters k_{obs}, the concentration of MCH, MC and SP, the achieved photoisomerization to SP as well as the equilibrium with water, K_w (details SI-S11). At high initial pH values (~pK_a) the model reproduces the experimental line shape, time scale and pH recovery values exceptionally well. At low pH values the line shape and final pH values match well but the predicted timescales of the pH recovery process are slightly faster than the experimental data.

Very small changes in concentrations and the many interlinked equilibrium processes make these systems highly sensitive to small changes and challenging to model. Nonetheless, we can see that depending on the initial pH, the recovery of the same photoacid (**3d**) varied by almost one order of magnitude ($pH_{initial}$ 6.98: apparent $t_{1/2}$ ~1.4 min, $pH_{initial}$ 5.20: apparent $t_{1/2}$ ~9.3 min) over the same pH

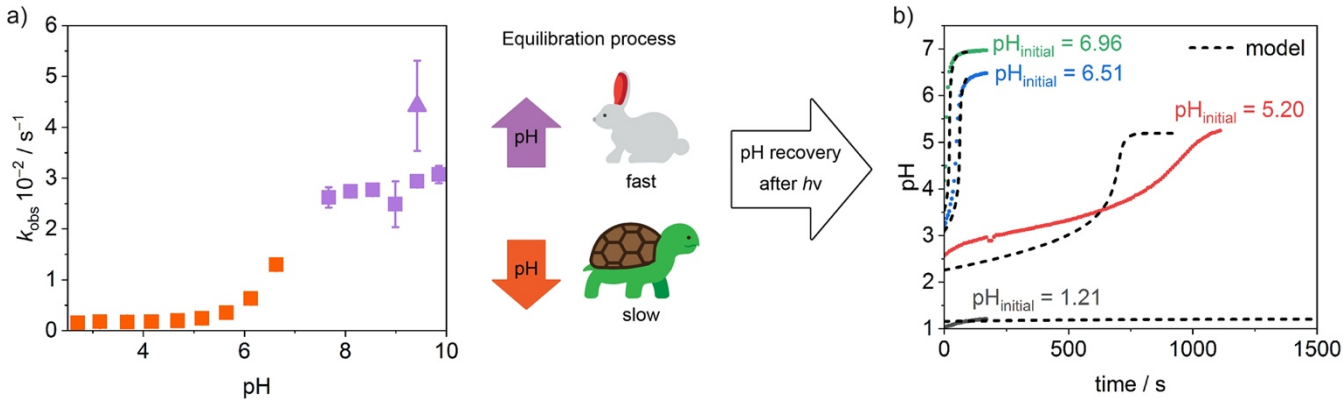

Figure 6. a) Observed rate constants k_{obs} over the pH range of photoacid **3d** for the thermal equilibration of MC ⇌ SP. Samples at different pH values were measured in 20 mM phosphate buffer to ensure the pH was constant during the isomerization. Rate constants were obtained from a first order exponential fit to the change in the characteristic absorbance peak (orange: MCH, purple: MC) over time after the equilibrium was perturbed (boxes: change in pH, triangle: after 265 nm light irradiation see SI-S5.3, S5.6). b) The pH recovery in the dark of a concentrated solution of **3d** after blue light irradiation (λ = 450 nm), initial pH values before irradiation are indicated and the respective prediction of the model is shown as dashed lines.

range, as estimated from the data in Figure 6b. The nonlinear behavior of the system and pH-tunability could give rise to interesting applications. Implementation of switching cycles which do not allow full recovery could enable fast cycling, for example between pH 5 and 6, by timing the irradiation and recovery time of the system. Modifying the speed of pH recovery could also open up new opportunities, for example in gel research where control over the pH tunes the properties of the gel.

Finally, we demonstrated the reversibility of visible light induced pH switching of photoacid **3d** at reasonable timescales (2-3 min per cycle at ambient temperature). Photoacid **3d** has the highest reported pK_a^{dark} value (5.56) of the alkylammonium spiropyran derivatives and combined with its good solubility we were able to switch the pH of a solution by ~3.2 units from pH 6.5 to pH 3.3 over 16 cycles without showing significant decomposition (Fig 7, loss of ΔpH = 0.1). By comparison, photoacid **2a** and its analog with a butyl sulfonate chain (**5**) have achieved pH switching of ~2 and 2.5 units respectively.[16a,31] A very recent report of a related methoxy derivative increased this pH switching to 3 units.[32]

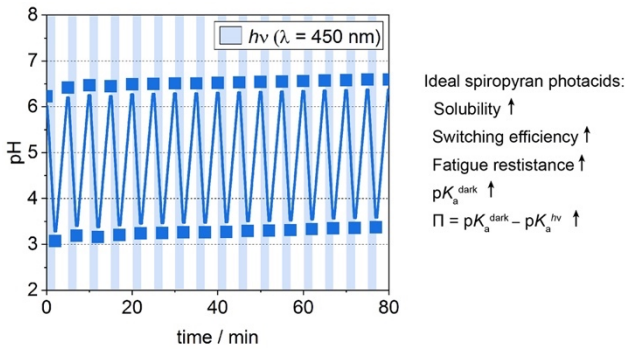

Figure 7. Visible light induced (λ = 450 nm, indicated by blue boxes) pH switching of a concentrated solution of photoacid **3d** (~8 mM) by ~3.2 units over 16 cycles (left). Highlighting key parameters of spiropyran photoacids to optimize light induced pH switching (right).

CONCLUSIONS

In conclusion, we report crucial parameters describing the photoacidic behavior (pK_a^{dark}, $pK_a^{h\nu}$) and kinetic parameters for spiropyran photoacids **2b–c**, **3a–d** to show how their behavior can be predicted. Comparison with the literature provides understanding of electronic effects influencing these parameters providing clear guidelines for future designs. The photoacidity appears to be consistent regardless of the substitution pattern.

We identified that increasing pK_a^{dark} values and operating the spiropyran photoacids at higher pH values maximized the achievable light-induced pH changes. The upper pH operating range is limited by the pK_a^{dark} value and the autoionization of water. The solubility also plays a crucial role in changing bulk pH values with alkylammonium spiropyrans being more soluble than alkylsulfonate derivatives. The qualitative model we developed allows prediction of light-induced pH changes based on the concentration, pK_a^{dark} and $pK_a^{h\nu}$ values that can be applied to many spiropyran photoacids (see SI-S10.5). Specific reversible pH changes can be accessed by choosing a suitable photoacid making spiropyran photoacids an incredibly useful tool for generating custom pH changes with visible light. The rate of pH recovery in the dark after visible light irradiation can also be adjusted as this process is nonlinear due to the pH dependence of the observed rate constant. By choosing specific pH operating ranges and photoacids with varying pK_a^{dark} values the time of pH recovery in the dark can be tuned.

Finally, we were able to increase the light-induced pH change of spiropyran photoacids to ~3.2 units (pH 6.5 to pH 3.3) using photoacid **3d** with high reversibility. Tuning the scale of pH switching at different pH ranges and controlling the timescales of switching will improve control over pH responsive systems and offers exciting new possibilities in any research area that applies pH to control chemical or biological processes, including using photoswitches to drive systems away from equilibrium.[44]

ASSOCIATED CONTENT

Synthetic procedures, spectroscopic data, all photoswitching and fitted data available in the Supporting Information. This material is available free of charge via the Internet at http://pubs.acs.org. All associated data for this work is freely available on the ChemRxiv server, DOI: 10.33774/chemrxiv-2021-gppx1.

AUTHOR INFORMATION

Corresponding Author

* Jonathon E. Beves j.beves@unsw.edu.au

Authors

† School of Chemistry, UNSW Sydney, Sydney NSW 2052, Australia

‡ Department of Chemistry and Chemical Engineering, Chalmers University of Technology, 412 96 Göteborg, Sweden

Funding Sources

We thank the Australian Research Council (JEB, FT170100094) for funding support.

Notes

The authors declare no competing financial interests.

ACKNOWLEDGMENT

This work was supported by the Australian Research Council (JEB: FT170100094; TWS, SKKP, JEB: Centre of Excellence in Exciton Science CE170100026). We acknowledge the Mark Wainwright Analytical Centre at UNSW Sydney, for access to the NMR facility.

REFERENCES

(1) (a) Hull, J. F.; Himeda, Y.; Wang, W.-H.; Hashiguchi, B.; Periana, R.; Szalda, D. J.; Muckerman, J. T.; Fujita, E. Reversible hydrogen storage using CO_2 and a proton-switchable iridium catalyst in aqueous media under mild temperatures and pressures. *Nat. Chem* **2012**, *4*, 383-388; (b) Geri, J. B.; Szymczak, N. K. A Proton-Switchable Bifunctional Ruthenium Complex That Catalyzes Nitrile Hydroboration. *J. Am. Chem. Soc.* **2015**, *137*, 12808-12814; (c) Semwal, S.; Choudhury, J. Molecular Coordination-Switch in a New Role: Controlling Highly Selective Catalytic Hydrogenation with Switchability Function. *ACS Catal.* **2016**, *6*, 2424-2428; (d) Blyth, M. T.; Coote, M. L. A pH-Switchable Electrostatic Catalyst for the Diels–Alder Reaction: Progress toward Synthetically Viable Electrostatic Catalysis. *J. Org. Chem.* **2019**, *84*, 1517-1522; (e) Arlegui, A.; Torres, P.; Cuesta, V.; Crusats, J.; Moyano, A. A pH-Switchable Aqueous Organocatalysis with Amphiphilic Secondary Amine–Porphyrin Hybrids. *Eur. J. Org. Chem.* **2020**, *2020*, 4399-4407.

(2) (a) Branda, N.; Grotzfeld, R. M.; Valdes, C.; Rebek, J., Jr. Control of Self-Assembly and Reversible Encapsulation of Xenon in a Self-Assembling Dimer by Acid-Base Chemistry. *J. Am. Chem. Soc.* **1995**, *117*, 85-88; (b) Ibukuro, F.; Kusukawa, T.; Fujita, M. A Thermally Switchable Molecular Lock. Guest-Templated Synthesis of a Kinetically Stable Nanosized Cage. *J. Am. Chem. Soc.* **1998**, *120*, 8561-8562; (c) Grote, Z.; Scopelliti, R.; Severin, K. pH-Triggered Assembly of Organometallic Receptors for Lithium Ions. *J. Am. Chem. Soc.* **2004**, *126*, 16959-16972; (d) Gottschalk, T.; Jaun, B.; Diederich, F. Container Molecules with Portals: Reversibly Switchable Cycloalkane Complexation. *Angew. Chem. Int. Ed.* **2007**, *46*, 260-264; (e) Mal, P.; Schultz, D.; Beyeh, K.; Rissanen, K.; Nitschke, J. R. An Unlockable–Relockable Iron Cage by Subcomponent Self-Assembly. *Angew. Chem. Int. Ed.* **2008**, *47*, 8297-8301; (f) Carvalho, C. P.; Uzunova, V. D.; Da Silva, J. P.; Nau, W. M.; Pischel, U. A photoinduced pH jump applied to drug release from cucurbit[7]uril. *Chem. Commun.* **2011**, *47*, 8793-8795; (g) Isaacs, L. Stimuli Responsive Systems Constructed Using Cucurbit[n]uril-Type Molecular Containers. *Acc. Chem. Res.* **2014**, *47*, 2052-2062; (h) Altmann, P. J.; Pöthig, A. A pH-Dependent, Mechanically Interlocked Switch: Organometallic [2]Rotaxane vs. Organic [3]Rotaxane. *Angew. Chem. Int. Ed.* **2017**, *56*, 15733-15736.

(3) (a) Bruns, C. J.; Stoddart, J. F. Rotaxane-Based Molecular Muscles. *Acc. Chem. Res.* **2014**, *47*, 2186-2199; (b) Zhou, H. Y.; Han, Y.; Chen, C. F. pH-Controlled motions in mechanically interlocked molecules. *Mater. Chem. Phys.* **2020**, *4*, 12-28; (c) Rizzuto, F. J.; Platnich, C. M.; Luo, X.; Shen, Y.; Dore, M. D.; Lachance-Brais, C.; Guarne, A.; Cosa, G.; Sleiman, H. F. A dissipative pathway for the structural evolution of DNA fibres. *Nat. Chem.* **2021**, 10.1038/s41557-021-00751-w.

(4) (a) Bissell, R. A.; Cordova, E.; Kaifer, A. E.; Stoddart, J. F. A chemically and electrochemically switchable molecular shuttle. *Nature* **1994**, *369*, 133-137; (b) Ashton, P. R.; Ballardini, R.; Balzani, V.; Baxter, I.; Credi, A.; Fyfe, M. C. T.; Gandolfi, M. T.; Gómez-López, M.; Martínez-Díaz, M. V.; Piersanti, A.; Spencer, N.; Stoddart, J. F.; Venturi, M.; White, A. J. P.; Williams, D. J. Acid–Base Controllable Molecular Shuttles. *J. Am. Chem. Soc.* **1998**, *120*, 11932-11942; (c) Crowley, J. D.; Leigh, D. A.; Lusby, P. J.; McBurney, R. T.; Perret-Aebi, L.-E.; Petzold, C.; Slawin, A. M. Z.; Symes, M. D. A Switchable Palladium-Complexed Molecular Shuttle and Its Metastable Positional Isomers. *J. Am. Chem. Soc.* **2007**, *129*, 15085-15090.

(5) Irie, M. Light-induced reversible pH change. *J. Am. Chem. Soc.* **1983**, *105*, 2078-2079.

(6) (a) Pines, E.; Huppert, D.; Agmon, N. Geminate recombination in excited-state proton-transfer reactions: Numerical solution of the Debye–Smoluchowski equation with backreaction and comparison with experimental results. *J. Chem. Phys.* **1988**, *88*, 5620-5630; (b) Spies, C.; Finkler, B.; Acar, N.; Jung, G. Solvatochromism of pyranine-derived photoacids. *Phys. Chem. Chem. Phys.* **2013**, *15*, 19893-19905.

(7) Also reported as 7.8 vs 0.4, see Pines, E.; Huppert, D. pH jump: a relaxational approach. *J. Phys. Chem.* **1983**, *87*, 4471-4478.

(8) (a) Yucknovsky, A.; Mondal, S.; Burnstine-Townley, A.; Foqara, M.; Amdursky, N. Use of Photoacids and Photobases To Control Dynamic Self-Assembly of Gold Nanoparticles in Aqueous and Nonaqueous Solutions. *Nano Lett.* **2019**, *19*, 3804-3810; (b) Legrand, A.; Liu, L.-H.; Royla, P.; Aoyama, T.; Craig, G. A.; Carné-Sánchez, A.; Urayama, K.; Weigand, J. J.; Lin, C.-H.; Furukawa, S. Spatiotemporal Control of Supramolecular Polymerization and Gelation of Metal–Organic Polyhedra. *J. Am. Chem. Soc.* **2021**, *143*, 3562-3570.

(9) Significant pK_a changes have been reported for azobenzene-type switches, see (a) Beharry, A. A.; Sadovski, O.; Woolley, G. A. Azobenzene Photoswitching without Ultraviolet Light. *J. Am. Chem. Soc.* **2011**, *133*, 19684-19687; (b) Emond, M.; Sun, J.; Grégoire, J.; Maurin, S.; Tribet, C.; Jullien, L. Photoinduced pH drops in water. *Phys. Chem. Chem. Phys.* **2011**, *13*, 6493-6499; (c) Weston, C. E.; Richardson, R. D.; Fuchter, M. J. Photoswitchable basicity through the use of azoheteroarenes. *Chem. Commun.* **2016**, *52*, 4521-4524; (d) Kennedy, A. D. W.; Sandler, I.; Andréasson, J.; Ho, J.; Beves, J. E. Visible-Light Photoswitching by Azobenzazoles. *Chem.– Eur. J.* **2020**, *26*, 1103-1110; (e) Ludwanowski, S.; Ari, M.; Parison, K.; Kalthoum, S.; Straub, P.; Pompe, N.; Weber, S.; Walter, M.; Walther, A. pH Tuning of Water-Soluble Arylazopyrazole Photoswitches. *Chem.– Eur. J.* **2020**, *26*, 13203-13212. For an example of pK_a changes of an azobenzene-type switch with pK_a: *E* 7.2; *Z* 5.7, see (f) Samanta, S.; Babalhavaeji, A.; Dong, M.-X.; Woolley, G. A. Photoswitching of *ortho*-Substituted Azonium Ions by Red Light in Whole Blood. *Angew. Chem. Int. Ed.* **2013**, *52*, 14127-14130. For an example of pK_a changes with an azobenzene-type switch of pK_a: *E* 4.7, *Z* 6.0, see (c). For examples of pK_a switching using diarylethenes, see (g) Kawai, S. H.; Gilat, S. L.; Lehn, J.-M. Photochemical pK_a-Modulation and Gated Photochromic Properties of a Novel Diarylethene Switch. *Eur. J. Org. Chem.* **1999**, *1999*,

2359-2366; (h) Massaad, J.; Micheau, J.-C.; Coudret, C.; Sanchez, R.; Guirado, G.; Delbaere, S. Gated Photochromism and Acidity Photomodulation of a Diacid Dithienylethene Dye. *Chem.– Eur. J.* **2012**, *18*, 6568-6575. For an example of a diarylethene with pK_a: open 10.2, closed 9.0, see (i) Odo, Y.; Matsuda, K.; Irie, M. pK_a Switching Induced by the Change in the π-Conjugated System Based on Photochromism. *Chem.– Eur. J.* **2006**, *12*, 4283-4288. For a diarylethene with pK_a open 4.0, closed 6.8, see (j) Gurke, J.; Budzák, Š.; Schmidt, B. M.; Jacquemin, D.; Hecht, S. Efficient Light-Induced pK_a-Modulation Coupled to Base-Catalyzed Photochromism. *Angew. Chem. Int. Ed.* **2018**, *57*, 4797-4801. For pK_a switching with hemithioindigos with pK_a: *trans* 7.2, *cis* 5.0, see (k) Koeppe, B.; Rühl, S.; Römpp, F. Towards More Effective, Reversible pH Control by Visible Light Alone: A Thioindigo Photoswitch Undergoing a Strong pK_a Modulation by Isomer-Specific Hydrogen Bonding. *ChemPhotoChem* **2019**, *3*, 71-74. For pK_a switching using nitrile-rich photoswitches with pK_a: closed 3.9, open 6.6, see (l) Belikov, M. Y.; Ievlev, M. Y.; Bardasov, I. N. A novel water-soluble multicolor halo- and photochromic switching system based on a nitrile-rich acceptor. *New J. Chem.* **2021**, *45*, 10287-10295.

(10) (a) Klajn, R. Spiropyran-based dynamic materials. *Chem. Soc. Rev.* **2014**, *43*, 148-184; (b) Kortekaas, L.; Browne, W. R. The evolution of spiropyran: fundamentals and progress of an extraordinarily versatile photochrome. *Chem. Soc. Rev.* **2019**, *48*, 3406-3424.

(11) (a) Raymo, F. M.; Giordani, S. Signal Processing at the Molecular Level. *J. Am. Chem. Soc.* **2001**, *123*, 4651-4652; (b) Raymo, F. M.; Giordani, S.; White, A. J. P.; Williams, D. J. Digital Processing with a Three-State Molecular Switch. *J. Org. Chem.* **2003**, *68*, 4158-4169.

(12) Silvi, S.; Arduini, A.; Pochini, A.; Secchi, A.; Tomasulo, M.; Raymo, F. M.; Baroncini, M.; Credi, A. A Simple Molecular Machine Operated by Photoinduced Proton Transfer. *J. Am. Chem. Soc.* **2007**, *129*, 13378-13379.

(13) (a) Silvi, S.; Constable, E. C.; Housecroft, C. E.; Beves, J. E.; Dunphy, E. L.; Tomasulo, M.; Raymo, F. M.; Credi, A. Photochemical switching of luminescence and singlet oxygen generation by chemical signal communication. *Chem. Commun.* **2009**, 1484-1486; (b) Silvi, S.; Constable, E. C.; Housecroft, C. E.; Beves, J. E.; Dunphy, E. L.; Tomasulo, M.; Raymo, F. M.; Credi, A. All-Optical Integrated Logic Operations Based on Chemical Communication between Molecular Switches. *Chem.– Eur. J.* **2009**, *15*, 178-185.

(14) Raymo, F. M.; Giordani, S. Signal Communication between Molecular Switches. *Org. Lett.* **2001**, *3*, 3475-3478.

(15) Miskolczy, Z.; Biczók, L. Photochromism in Cucurbit[8]uril Cavity: Inhibition of Hydrolysis and Modification of the Rate of Merocyanine–Spiropyran Transformations. *J. Phys. Chem. B* **2011**, *115*, 12577-12583.

(16) (a) Shi, Z.; Peng, P.; Strohecker, D.; Liao, Y. Long-Lived Photoacid Based upon a Photochromic Reaction. *J. Am. Chem. Soc.* **2011**, *133*, 14699-14703; (b) Liao, Y. Design and Applications of Metastable-State Photoacids. *Acc. Chem. Res.* **2017**, *50*, 1956-1964.

(17) The analogue that includes the *para*-NO_2 group has a pK_a in the dark of 6.36, around 1.5 units higher than **2a**, see Ref. 16a.

(18) (a) Shi, Q.; Chen, C. F. Switchable Complexation between (O-Methyl)6-2,6-helic[6]arene and Protonated Pyridinium Salts Controlled by Acid/Base and Photoacid. *Org. Lett.* **2017**, *19*, 3175-3178; (b) Jansze, S. M.; Cecot, G.; Severin, K. Reversible disassembly of metallasupramolecular structures mediated by a metastable-state photoacid. *Chem. Sci.* **2018**, *9*, 4253-4257; (c) Kothapalli, S. S. K.; Kannekanti, V. K.; Ye, Z. C.; Yang, Z. Y.; Chen, L. X.; Cai, Y. M.; Zhu, B. C.; Feng, W.; Yuan, L. H. Light-controlled switchable complexation by a non-photoresponsive hydrogen-bonded amide macrocycle. *Org. Chem. Frontiers* **2020**, *7*, 846-855; (d) Li, R.-J.; Pezzato, C.; Berton, C.; Severin, K. Light-induced assembly and disassembly of polymers with PdnL2n-type network junctions. *Chem. Sci.* **2021**, *12*, 4981-4984.

(19) (a) Guo, J.; Zhang, H. Y.; Zhou, Y.; Liu, Y. Light-controlled reversible self-assembly of nanorod suprastructures. *Chem. Commun.* **2017**, *53*, 6089-6092; (b) Cissé, N.; Kudernac, T. Light-Fuelled Self-Assembly of Cyclic Peptides into Supramolecular Tubules. *ChemSystemsChem* **2020**, *2*, e2000012; (c) Chen, X.-M.; Hou, X.-F.; Bisoyi, H. K.; Feng, W.-J.; Cao, Q.; Huang, S.; Yang, H.; Chen, D.; Li, Q. Light-fueled transient supramolecular assemblies in water as fluorescence modulators. *Nat. Commun.* **2021**, *12*, 4993.

(20) Ryssy, J.; Natarajan, A. K.; Wang, J.; Lehtonen, A. J.; Nguyen, M. K.; Klajn, R.; Kuzyk, A. Light-Responsive Dynamic DNA-Origami-Based Plasmonic Assemblies. *Angew. Chem.* **2021**, *60*, 5859-5863.

(21) For an example using the *N*-Me spiropyran deriviative instead of **2a**, see Kundu, P. K.; Samanta, D.; Leizrowice, R.; Margulis, B.; Zhao, H.; Börner, M.; Udayabhaskararao, T.; Manna, D.; Klajn, R. Light-controlled self-assembly of non-photoresponsive nanoparticles. *Nat. Chem* **2015**, *7*, 646-652.

(22) (a) Moreno, S.; Sharan, P.; Engelke, J.; Gumz, H.; Boye, S.; Oertel, U.; Wang, P.; Banerjee, S.; Klajn, R.; Voit, B.; Lederer, A.; Appelhans, D. Light-Driven Proton Transfer for Cyclic and Temporal Switching of Enzymatic Nanoreactors. *Small* **2020**, *16*, 2002135; (b) For an example using the *para*-NO_2 spiropyran derviative bridging polymers, see Qu, P.; Kuepfert, M.; Hashmi, M.; Weck, M. Compartmentalization and Photoregulating Pathways for Incompatible Tandem Catalysis. *J. Am. Chem. Soc.* **2021**, *143*, 4705-4713.

(23) For an example using the *para*-NO_2 spiropyran derviative attached to a polymer via a linker from the amine, see Li, C.; Iscen, A.; Sai, H.; Sato, K.; Sather, N. A.; Chin, S. M.; Álvarez, Z.; Palmer, L. C.; Schatz, G. C.; Stupp, S. I. Supramolecular–covalent hybrid polymers for light-activated mechanical actuation. *Nat. Mater.* **2020**, *19*, 900-909.

(24) (a) Maity, C.; Hendriksen, W. E.; van Esch, J. H.; Eelkema, R. Spatial Structuring of a Supramolecular Hydrogel by using a Visible-Light Triggered Catalyst. *Angew. Chem. Int. Ed.* **2015**, *54*, 998-1001; (b) Li, X.; Fei, J.; Xu, Y.; Li, D.; Yuan, T.; Li, G.; Wang, C.; Li, J. A Photoinduced Reversible Phase Transition in a Dipeptide Supramolecular Assembly. *Angew. Chem. Int. Ed.* **2018**, *57*, 1903-1907.

(25) Zhang, T.; Sheng, L.; Liu, J.; Ju, L.; Li, J.; Du, Z.; Zhang, W.; Li, M.; Zhang, S. X.-A. Photoinduced Proton Transfer between Photoacid and pH-Sensitive Dyes: Influence Factors and Application for Visible-Light-Responsive Rewritable Paper. *Adv. Funct. Mater.* **2018**, *28*, 1705532.

(26) Fu, C.; Xu, J.; Boyer, C. Photoacid-mediated ring opening polymerization driven by visible light. *Chem. Commun.* **2016**, *52*, 7126-7129.

(27) Tatum, L. A.; Foy, J. T.; Aprahamian, I. Waste management of chemically activated switches: using a photoacid to eliminate accumulation of side products. *J. Am. Chem. Soc.* **2014**, *136*, 17438-17441.

(28) Xu, Y.; Fei, J.; Li, G.; Yuan, T.; Li, Y.; Wang, C.; Li, X.; Li, J. Enhanced Photophosphorylation of a Chloroplast-Entrapping Long-Lived Photoacid. *Angew. Chem. Int. Ed.* **2017**, *56*, 12903-12907.

(29) Shi, Q.; Meng, Z.; Xiang, J.-F.; Chen, C.-F. Efficient control of movement in non-photoresponsive molecular machines by a photo-induced proton-transfer strategy. *Chem. Commun.* **2018**, *54*, 3536-3539.

(30) Vallet, J.; Micheau, J. C.; Coudret, C. Switching a pH indicator by a reversible photoacid: A quantitative analysis of a new two-component photochromic system. *Dyes Pigm.* **2016**, *125*, 179-184.

(31) Berton, C.; Busiello, D. M.; Zamuner, S.; Solari, E.; Scopelliti, R.; Fadaei-Tirani, F.; Severin, K.; Pezzato, C. Thermodynamics and kinetics of protonated merocyanine photoacids in water. *Chem. Sci.* **2020**, *11*, 8457-8468.

(32) Berton, C.; Busiello, D. M.; Zamuner, S.; Scopelliti, R.; Fadaei-Tirani, F.; Severin, K.; Pezzato, C. Light-switchable buffers. *Angew. Chem. Int. Ed.* **2021**, https://doi.org/10.1002/anie.202109250.

(33) (a) Hammarson, M.; Nilsson, J. R.; Li, S.; Beke-Somfai, T.; Andréasson, J. Characterization of the Thermal and Photoinduced

Reactions of Photochromic Spiropyrans in Aqueous Solution. *J. Phys. Chem. B* **2013**, *117*, 13561-13571; (b) Abeyrathna, N.; Liao, Y. Stability of merocyanine-type photoacids in aqueous solutions. *J. Phys. Org. Chem.* **2017**, *30*, e3664.

(34) Fleming, C. L.; Li, S.; Grøtli, M.; Andréasson, J. Shining New Light on the Spiropyran Photoswitch: A Photocage Decides between cis–trans or Spiro-Merocyanine Isomerization. *J. Am. Chem. Soc.* **2018**, *140*, 14069-14072.

(35) Aldaz, C. R.; Wiley, T. E.; Miller, N. A.; Abeyrathna, N.; Liao, Y.; Zimmerman, P. M.; Sension, R. J. Experimental and Theoretical Characterization of Ultrafast Water-Soluble Photochromic Photoacids. *J. Phys. Chem. B* **2021**, *125*, 4120-4131.

(36) Kortekaas, L.; Chen, J.; Jacquemin, D.; Browne, W. R. Proton-Stabilized Photochemically Reversible E/Z Isomerization of Spiropyrans. *J. Phys. Chem. B* **2018**, *122*, 6423-6430.

(37) Liu, J.; Tang, W.; Sheng, L.; Du, Z.; Zhang, T.; Su, X.; Zhang, S. X.-A. Effects of Substituents on Metastable-State Photoacids: Design, Synthesis, and Evaluation of their Photochemical Properties. *Chem.– Asian J.* **2019**, *14*, 438-445.

(38) Kaiser, C.; Halbritter, T.; Heckel, A.; Wachtveitl, J. Proton-Transfer Dynamics of Photoacidic Merocyanines in Aqueous Solution. *Chem.– Eur. J.* **2021**, *27*, 9160-9173.

(39) For a detailed discussion of the identification of cis-MCH, see Browne et al.

(40) (a) Satoh, T.; Sumaru, K.; Takagi, T.; Takai, K.; Kanamori, T. Isomerization of spirobenzopyrans bearing electron-donating and electron-withdrawing groups in acidic aqueous solutions. *Phys. Chem. Chem. Phys.* **2011**, *13*, 7322-7329; (b) Moldenhauer, D.; Gröhn, F. Water-Soluble Spiropyrans with Inverse Photochromism and Their Photoresponsive Electrostatic Self-Assembly. *Chem.– Eur. J.* **2017**, *23*, 3966-3978.

(41) Johns, V. K.; Wang, Z.; Li, X.; Liao, Y. Physicochemical Study of a Metastable-State Photoacid. *J. Phys. Chem. A* **2013**, *117*, 13101-13104.

(42) Kaiser, C.; Halbritter, T.; Heckel, A.; Wachtveitl, J. Thermal, Photochromic and Dynamic Properties of Water-Soluble Spiropyrans. *ChemistrySelect* **2017**, *2*, 4111-4123.

(43) Zhang, Y.; Ng, M.; Hong, E. Y.-H.; Chan, A. K.-W.; Wu, N. M.-W.; Chan, M. H.-Y.; Wu, L.; Yam, V. W.-W. Synthesis and photoswitchable amphiphilicity and self-assembly properties of photochromic spiropyran derivatives. *J. Mater. Chem. C* **2020**, *8*, 13676-13685.

(44) (a) Kathan, M.; Hecht, S. Photoswitchable molecules as key ingredients to drive systems away from the global thermodynamic minimum. *Chem. Soc. Rev.* **2017**, *46*, 5536-5550; (b) Andréasson, J.; Pischel, U. Light-stimulated molecular and supramolecular systems for information processing and beyond. *Coord. Chem. Rev.* **2021**, *429*, 213695.